Mutual Coupling of Antennas With Overlapping Minimum Spheres Based on the Transformation Between Spherical and Plane Vector Waves

Jesús Rubio and Rafael Gómez-Alcalá, *Member, IEEE*

***Abstract*— Mutual coupling in finite arrays of antennas with strongly overlapping minimum spheres is quickly calculated by computing the general translation matrix between spherical modes. This matrix is obtained by using the transformation properties of spherical and plane vector waves. Although this approach is less efficient than the classical one, which is based on addition theorems, it allows to overcome the well-known limitation of addition theorems that requires nonintersecting minimum spheres. Symmetry relations are provided for the translation coefficients that greatly increase the speed of computation of the general translation matrix. By computing the reflection and the transmission submatrices of the generalized scattering matrix of a finite antenna array, accurate results are obtained for the S-parameters and the radiation patterns of arrays, in comparison with commercial software or a purely numerical in-house full-wave method. For this purpose, different types of antennas with strongly overlapping hemispheres in an array environment on a ground plane are used, such as apertures, monopoles, cavity-backed patch antennas, or dielectric resonator antennas.**

***Index Terms*— Addition theorems, finite arrays, generalized scattering matrix (GSM), mutual coupling, plane wave expansion, spherical wave expansion.**

I. Introduction

TRANSLATION of spherical vector waves (spherical modes) has been widely used for decades for the efficient study of electromagnetic scattering by particle groups [1], [2] (and its updates [3] and references therein), in spherical near-field antenna measurements with probe correction [4] or, more recently, for the fast analysis of finite antenna arrays [5]–[7]. Most of these works are based on computing this translation by applying addition theorems for spherical waves [8], [9], as it is a purely analytical method. However, it is well known that addition theorems are not strictly valid when the minimum possible sphere circumscribing the antenna overlaps the minimum possible sphere circumscribing the other antenna [4]. Consequently, the method proposed in [5]–[7] cannot be used directly for the analysis of finite arrays with elongated elements that are very close to each other, since addition theorems are used to couple spherical modes between elements.

In order to overcome this limitation, a full-wave antenna modeling method by means of infinitesimal dipoles was presented in [10] and [11] for planar and volumetric antennas, respectively. These works took advantage of the ability of equivalent dipoles to synthesize the field within the minimum sphere of the antenna [12]. Thus, after obtaining the antenna model, the array response can be calculated by coupling the equivalent dipoles using addition theorems, since they correspond to lower order spherical modes. However, the major drawback of this method is that it requires obtaining an accurate model of the antenna through an optimization method. In addition, from distances between antenna edges less than 0.15λ to 0.2λ the method starts to lose accuracy.

Alternatively to the translation of spherical modes based on addition theorems of spherical vector waves, it was established in [13] that such translation could be carried out by using transformation properties between spherical waves and plane waves, and translation of the latter. Although this procedure has no apparent advantages over the use of addition theorems, since it requires numerical integration, it has been recently shown in [14] that it can be used for the computation of light scattering of spheroidal particles with strongly overlapping minimum spheres.

In this work, the translation procedure based on the transformation to plane waves proposed in [13] is used for the efficient analysis of finite arrays of antennas with strongly overlapping minimum spheres. In addition, symmetry relations for the translation coefficients, which allow the computation time to be significantly reduced, are provided. Previously, the analysis of finite antenna arrays by means of the generalized scattering matrix (GSM) of a finite array, obtained from the GSM of isolated elements and translation of spherical modes, is briefly reviewed. Finally, some results are presented for different types of array elements that are intended to show the capabilities of the proposed method.

II. Theory

A. Analysis of Finite Arrays Based on Translation of Spherical Modes

The overall GSM of a finite array of N antennas in terms of spherical modes, including mutual coupling, can be defined as

$$\begin{bmatrix} \boldsymbol{\Gamma}_{\mathrm{G}} & \mathbf{R}_{\mathrm{G}} \\ \mathbf{T}_{\mathrm{G}} & \mathbf{S}_{\mathrm{G}}-\mathbf{I} \end{bmatrix} \begin{bmatrix} \mathbf{v} \\ \mathbf{a} \end{bmatrix} = \begin{bmatrix} \mathbf{w} \\ \mathbf{b} \end{bmatrix} \tag{1}$$

Manuscript received March 30, 2020; revised July 13, 2020; accepted August 30, 2020. Date of publication October 1, 2020; date of current version April 7, 2021. This work was supported in part by Ministerio de Economía y Competitividad (MINECO)/Agencia Estatal de Investigación (AEI)/Fondo Europeo de Desarrollo Regional (FEDER), Unión Europea (UE), Spain, under Project TEC2017-83352-C2-2-P and Project TEC2017-83352-C2-1-P and in part by the Junta de Extremadura and the FEDER Program (European Union) under Project GR18055. *(Corresponding author: Rafael Gómez-Alcalá.)*

The authors are with the Escuela Politécnica, Universidad de Extremadura, 10003 Cáceres, Spain (e-mail: jesusrubio@unex.es; rgomezal@unex.es).

Color versions of one or more of the figures in this article are available online at https://ieeexplore.ieee.org.

Digital Object Identifier 10.1109/TAP.2020.3026882

This work is licensed under a Creative Commons Attribution 4.0 License. For more information, see https://creativecommons.org/licenses/by/4.0/

with

$$\mathbf{v}=\begin{Bmatrix}\mathbf{v}_1\\ \vdots\\ \mathbf{v}_N\end{Bmatrix},\quad \mathbf{w}=\begin{Bmatrix}\mathbf{w}_1\\ \vdots\\ \mathbf{w}_N\end{Bmatrix},\quad \mathbf{a}=\begin{Bmatrix}\mathbf{a}_1\\ \vdots\\ \mathbf{a}_N\end{Bmatrix},\quad \mathbf{b}=\begin{Bmatrix}\mathbf{b}_1\\ \vdots\\ \mathbf{b}_N\end{Bmatrix} \tag{2}$$

where $\mathbf{v}_i$, $\mathbf{w}_i$, $\mathbf{a}_i$, and $\mathbf{b}_i$ are column vectors containing, respectively, the complex amplitudes of incident and reflected modes on the feeding ports, and the incoming and scattered spherical modes on the spherical ports, for the element i in the array. $\mathbf{I}$ is the identity matrix, and the submatrices $\mathbf{\Gamma}_\mathrm{G}$, $\mathbf{T}_\mathrm{G}$, $\mathbf{R}_\mathrm{G}$, and $\mathbf{S}_\mathrm{G}$, stand, respectively, for the reflection, reception, transmission, and scattering matrices of the finite array and are given by [5]

$$\begin{aligned}\mathbf{\Gamma}_\mathrm{G}&=\mathbf{\Gamma}+\mathbf{RG}[\mathbf{I}-(\mathbf{S}-\mathbf{I})\mathbf{G}]^{-1}\mathbf{T}\\ \mathbf{T}_\mathrm{G}&=[\mathbf{I}-(\mathbf{S}-\mathbf{I})\mathbf{G}]^{-1}\mathbf{T}\\ \mathbf{R}_\mathrm{G}&=\mathbf{R}+\mathbf{RG}[\mathbf{I}-(\mathbf{S}-\mathbf{I})\mathbf{G}]^{-1}(\mathbf{S}-\mathbf{I})\\ \mathbf{S}_\mathrm{G}-\mathbf{I}&=[\mathbf{I}-(\mathbf{S}-\mathbf{I})\mathbf{G}]^{-1}(\mathbf{S}-\mathbf{I})\end{aligned} \tag{3}$$

with

$$\begin{bmatrix}\Gamma & \mathbf{R}\\ \mathbf{T} & \mathbf{S}-\mathbf{I}\end{bmatrix}\begin{bmatrix}\mathbf{v}\\ \mathbf{a}\end{bmatrix}=\begin{bmatrix}\mathbf{w}\\ \mathbf{b}\end{bmatrix} \tag{4}$$

being the overall GSM of a finite array of N externally uncoupled antennas, in terms of spherical modes [5], [6]. For the usual case in which internal coupling does not exist, i.e., the feeding ports are uncoupled, Γ, $\mathbf{T}$, $\mathbf{R}$, and $\mathbf{S}$ will be diagonal block-matrices whose blocks will be the individual reflection, reception, transmission, and scattering matrices of each antenna i in isolation [5]. In (3), $\mathbf{G}$ is a square matrix that accounts for mutual coupling between the antennas in the array

$$\mathbf{G}=\begin{bmatrix}\mathbf{0} & \mathbf{G}_{21} & \cdots & \dots & \mathbf{G}_{1\ N}\\ \mathbf{G}_{21} & \mathbf{0} & \ddots & \mathbf{G}_{ij} & \vdots\\ \vdots & \ddots & \ddots & \ddots & \vdots\\ \vdots & \mathbf{G}_{ji} & \ddots & \mathbf{0} & \mathbf{G}_{N-1\ N}\\ \mathbf{G}_{N1} & \cdots & \dots & \mathbf{G}_{NN-1} & \mathbf{0}\end{bmatrix}. \tag{5}$$

The elements of $\mathbf{G}$ are general translation matrices between each pair of antennas i and j, obtained by rotation and translation of spherical modes, so that

$$\mathbf{a}_i^j=\mathbf{G}_{ij}\mathbf{b}_j. \tag{6}$$

In this way, the incoming field in antenna i from antenna j, expanded in terms of complex amplitudes of spherical modes $\mathbf{a}_i^j$, is obtained by means of translation of the scattered field by antenna j, expanded in terms of complex amplitudes of spherical modes $\mathbf{b}_j$.

Reflection matrix $\mathbf{\Gamma}_\mathrm{G}$ provides the S-parameters for feeding ports, i.e., the mutual coupling coefficients between them and the reflection coefficients taking into account mutual coupling effects.

By assuming no incident field coming from out of the array ($\mathbf{a}=\mathbf{0}$), the radiation pattern can be easily calculated from the transmission matrix $\mathbf{T}_\mathrm{G}$, given an excitation in terms of complex amplitudes of feeding modes $\mathbf{v}$, by applying superposition as

$$\mathbf{E}(\hat{u})=\left(\boldsymbol{e}(\hat{u})e^{-jk\hat{u}\cdot\boldsymbol{u}}\right)\mathbf{F}\mathbf{T}_\mathrm{G}\mathbf{v} \tag{7}$$

where

$$\left(\boldsymbol{e}(\hat{u})e^{-jk\hat{u}\cdot\boldsymbol{u}}\right)=\left(\boldsymbol{e}e^{-jk\hat{u}\cdot\boldsymbol{u_1}},\boldsymbol{e}e^{-jk\hat{u}\cdot\boldsymbol{u_2}},\dots,\boldsymbol{e}e^{-jk\hat{u}\cdot\boldsymbol{u_N}}\right) \tag{8}$$

k is the wavenumber in free space, $\hat{u}$ is the unitary vector in spherical coordinates, and $\boldsymbol{u}_i$ is the position vector of the array element i, $\boldsymbol{u}_i=x_i\hat{x}+y_i\hat{y}$. $\boldsymbol{e}$ is a row vector containing the electric fields of the spherical modes in each element, and $\mathbf{F}$ is a diagonal matrix that takes into account rotation angles in the case of rotated elements in the array [15].

B. General Translation Matrix Based on the Transformation Between Spherical and Plane Vector Waves

Alternatively to the translation of spherical modes based on addition theorems, it was established in [13] that it is possible to make such translation by means of a spherical to plane vector wave transformation and translation of the latter. The sequence of operations is as follows.

1) Express the field scattered by the antenna j in terms of spherical modes.
2) Expand each previous spherical mode in terms of plane vector waves in the z-axis direction of the spherical mode expansion.
3) Translate the plane vector waves from the antenna j to the antenna i, according to the propagation theory of plane vector waves, in the z-axis direction.
4) Expand each plane vector wave in terms of incoming spherical modes in the antenna i, so that the local z-axis in antenna i be parallel to the local z-axis of antenna j.

A priori, this approach has no advantages over the use of addition theorems, since step 2 results in a numerical integration of the plane wave spectrum, whereas the use of them only involves fully analytical calculations. However, as stated in [16], the plane vector wave expansion converges in the region where $z>z_{\min}$, with $z_{\min}$ being the largest z-coordinate of the antenna. This region is different from the convergence region of the expansion in spherical modes, given by $r>r_{\min}$, with $r_{\min}$ being the radius of the minimum sphere (or the hemisphere on a ground plane) that circumscribes the antenna. It should also be noted that $|z_{\min}|\leq r_{\min}$. Consequently, translation of spherical modes through a plane vector wave transformation can be carried out between two antennas, even if their minimum spheres overlap, when they are separated by a plane that does not intersect them. Such a plane will be perpendicular to the direction of propagation of plane vector waves.

This work is focused on planar arrays on a ground plane, so that we will assume that the separation plane is also orthogonal to the ground plane, which covers the vast majority of cases of this type of antenna arrays. Fig. 1 shows the geometric starting point for the general translation of spherical modes, where the local z-axes of the antennas (z' and z") are parallel. However, as mentioned above, translation based on the propagation of plane vector waves requires the z-axis to be perpendicular to the direction of propagation, which is defined by the separation plane. For this reason, a succession of rotations of spherical modes needs to be additionally carried out, to obtain the general translation matrix of spherical modes based on plane vector wave transformation. In this way, this

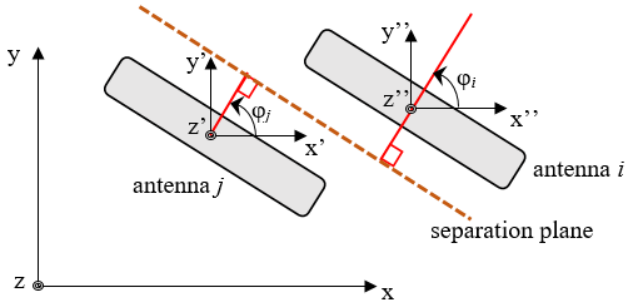

Fig. 1. Geometric approach for the general translation of spherical modes between two antennas on a ground plane based on plane vector wave transformation. Top view: ground plane is at z = 0.

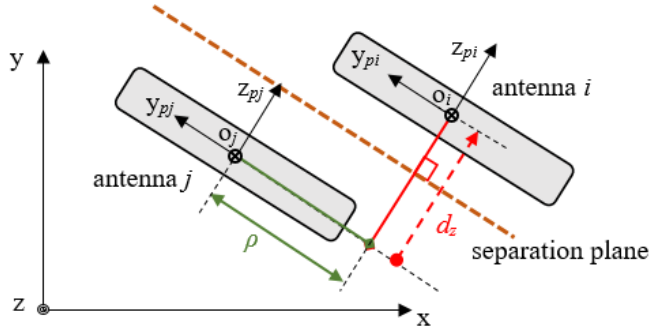

Fig. 2. Cylindrical coordinates of the center of antenna i, in the local coordinate systems of antennas j and i that allow the translation of spherical modes based on plane vector wave transformation. Top view.

matrix can be calculated as a product of matrices

$$\mathbf{G}_{ij} = \Big[\mathbf{R}_j(-\varphi_{rj})\mathbf{R}_j(\varphi_j)\mathbf{D}_j\Big(\frac{\pi}{2}\Big)\mathbf{Cp}(k, d_z, \rho, \phi) \times \mathbf{D}_i\Big(-\frac{\pi}{2}\Big)\mathbf{R}_i(-\varphi_i)\mathbf{R}_i(\varphi_{ri})\Big]^{\mathrm{T}}. \quad (9)$$

In (9), $\mathbf{R}_j(\varphi_j)$ is a diagonal matrix that performs a φ-rotation of the local coordinate system for antenna j (x',y',z'), so that the new x-axis points in the direction of propagation of plane vector waves. $\mathbf{D}_j(\pi/2)$ is a matrix that, starting from φ_j-rotated coordinate system for antenna j, performs a θ-rotation equal to $\pi/2$, so that the new z-axis points in the direction of propagation of plane vector waves. $\mathbf{Cp}(k, d_z, \rho, \phi)$ is the translation matrix of spherical modes, based on the transformation to plane vector waves and their propagation. On the other hand, $\mathbf{D}_i(-\pi/2)$ and $\mathbf{R}_i(-\varphi_i)$ perform the inverse rotations of coordinate systems for antenna i, so that the spherical modes refer to the local coordinate system for antenna i (x", y", z") after these rotations. $\mathbf{R}_j(-\varphi_{rj})$ and $\mathbf{R}_i(\varphi_{ri})$ are diagonal matrices that account for the local φ-rotations of antennas j and i, respectively, when their local coordinate systems, (x', y', z') and (x", y", z"), are not parallel to the global coordinate system of the array (x, y, z).

Additional details on this procedure, as well as the elements of matrices $\mathbf{D}$ and $\mathbf{R}$, can be found in [4] and [5].

The elements of $\mathbf{Cp}(k, d_z, \rho, \phi)$ can be computed by using the following expression, obtained after the sequence of operations 1)–4) described at the beginning of this section [13], [14]

$$\mathrm{Cp}_{s_i\mu_i n_i}^{s_j\mu_j n_j}(k, d_z, \rho, \phi) = 4(-\mathbf{j})^{|\mu_i-\mu_j|}e^{j\phi(\mu_i-\mu_j)} \times \sum_{p=1}^{2}\int d\kappa \frac{\kappa}{kk_z}\mathrm{B}_{jp}\Big(\frac{-k_z}{k}\Big)\mathrm{B}_{ip}^{\dagger}\Big(\frac{-k_z}{k}\Big)e^{-jk_z d_z}\mathrm{J}_{|\mu_i-\mu_j|}(\kappa\rho). \quad (10)$$

In (10), $\mathbf{j} = \sqrt{-1}$, κ is the in-plane wavenumber (the radial cylindrical coordinate of the wave propagation vector k), $k_z = \sqrt{k^2 - \kappa^2}$, $\mathrm{J}_{|\mu_i-\mu_j|}(\kappa\rho)$ is the Bessel function of the first kind and its order is the absolute value of $\mu_i - \mu_j$. B_{mp} $(m = j, i)$ is the transformation operator given by

$$\mathrm{B}_{mp}(\cos\vartheta) = \frac{-(\mathbf{j}\delta_{p1} + \delta_{p2})\Big(\delta_{s_m p}\frac{\partial P_{n_m}^{\mu_m}(\cos\vartheta)}{\partial\vartheta} + (1-\delta_{s_m p})\mu_m\frac{P_{n_m}^{\mu_m}(\cos\vartheta)}{\sin\vartheta}\Big)}{\mathbf{j}^{(n_m+1)}\sqrt{(2n_m+1)}} \quad (11)$$

where $P_{n_m}^{\mu_m}(\cos\vartheta)$ is the normalized associated Legendre function. In the "daggered" version (†), all explicit $\mathbf{j}$ are set to $(-\mathbf{j})$. Index s_m $(m = j, i)$ distinguishes with $s_m = 1$ and $s_m = 2$ between TE and TM spherical modes. Indices μ_m and n_m $(m = j, i)$ are the order and the degree of the spherical modes in the local coordinate systems of antennas j $(\mathrm{x}_{pj}, \mathrm{y}_{pj}, \mathrm{z}_{pj})$ and i $(\mathrm{x}_{pi}, \mathrm{y}_{pi}, \mathrm{z}_{pi})$, respectively, obtained after performing rotations. (d_z, ρ, ϕ) are the cylindrical coordinates of the antenna i center o_i, in the antenna j $(\mathrm{x}_{pj}, \mathrm{y}_{pj}, \mathrm{z}_{pj})$ local coordinate system, as shown in Fig. 2.

It should be noted that, since the antenna centers are in the same plane $(\mathrm{x}_{pi} = \mathrm{x}_{pj})$, ϕ can only be equal to $\pm\pi/2$.

The procedure just described in this section to compute the general translation matrix will be used only between pairs of antennas with minimal overlapping spheres. For the rest of pairs, the method proposed in [5] will be used, since it is more efficient as explained below.

C. Symmetry Properties of the Translation Coefficients

Computation of the general transmission matrix coefficients is more intensive when using a spherical modes translation based on plane vector waves propagation instead of addition theorems. The reason for this is that, in the latter case, calculations are analytical, the z-translation is always axial (z-axes are coaligned) and there are recurrence and symmetry relations that speed the computation [4], [5], [1]. In this sense, it should be noted that, for an axial translation, all the coefficients with $\mu_i \neq \mu_j$ vanish. This property can be also used in the case of plane vector waves propagation but it is only a particular case, although very usual in finite arrays, where the separation plane is orthogonal to the axial direction defined by the antenna centers ($\rho = 0$).

Despite this, computation of (10) can be significantly speeded-up by using symmetry properties. In this sense, we

have found the following relations:

$$\mathrm{Cp}^{s_i\mu_i n_i}_{s_j\mu_j n_j}(k,d_z,\rho,\phi) = e^{\mathrm{j}2\phi(\mu_j-\mu_i)}(-1)^{(n_i+n_j)} \times \mathrm{Cp}^{s_j\mu_j n_j}_{s_i\mu_i n_i}(k,d_z,\rho,\phi) \quad (12)$$

$$\mathrm{Cp}^{2\mu_j n_j}_{2\mu_i n_i}(k,d_z,\rho,\phi) = \mathrm{Cp}^{1\mu_j n_j}_{1\mu_i n_i}(k,d_z,\rho,\phi) \quad (13a)$$

$$\mathrm{Cp}^{1\mu_j n_j}_{2\mu_i n_i}(k,d_z,\rho,\phi) = \mathrm{Cp}^{2\mu_j n_j}_{1\mu_i n_i}(k,d_z,\rho,\phi) \quad (13b)$$

and

$$\mathrm{Cp}^{s_i\mu_i n_i}_{s_j\mu_j n_j}(k,d_z,\rho,\phi) = e^{\mathrm{j}2\phi(\mu_i-\mu_j)}(-1)^{(\mu_i-\mu_j)}(-1)^{(s_i+s_j)} \times \mathrm{Cp}^{s_j-\mu_j n_j}_{s_i-\mu_i n_i}(k,d_z,\rho,\phi). \quad (14)$$

Equation (12) allows to obtain the matrix **Cp** coefficients located above its diagonal from those below its diagonal or vice versa. Equation (13a) and (13b) provides the coefficients with $s_i = 2$ from the coefficients with $s_i = 1$. Finally, the coefficients with $\mu_i > 0$ can be computed from the coefficients with $\mu_i < 0$ by means of (14). In addition, since ϕ can only be equal to $\pm\pi/2$ in a planar array, (12) and (14) can be simplified

$$\mathrm{Cp}^{s_i\mu_i n_i}_{s_j\mu_j n_j}(k,d_z,\rho,\phi) = (-1)^{(\mu_j-\mu_i)}(-1)^{(n_i+n_j)} \times \mathrm{Cp}^{s_j\mu_j n_j}_{s_i\mu_i n_i}(k,d_z,\rho,\phi) \quad (15)$$

$$\mathrm{Cp}^{s_i\mu_i n_i}_{s_j\mu_j n_j}(k,d_z,\rho,\phi) = (-1)^{(s_i+s_j)}\mathrm{Cp}^{s_j-\mu_j n_j}_{s_i-\mu_i n_i}(k,d_z,\rho,\phi). \quad (16)$$

As an example, for a maximum value of n_i and n_j equal to 10 it is only necessary to compute 7700 coefficients. The rest up to 57 600 are quickly obtained from the previous ones using these symmetry relations. Moreover, in the particular case of an axial translation where the separation plane is orthogonal to the axial direction ($\rho = 0$), it is only necessary to compute 550 coefficients.

D. Number of Spherical Modes and Integral Truncation

The overall accuracy of translation matrix coefficients can be significantly degraded if the integral in (10) is truncated with a too large value, as shown in [17]. In that paper, a phenomenological formula that provides a conservative estimation of the maximum value of κ (κ_{tr}) was provided in the range of $0.5 \leq |kr_{\min}| \leq 10$ and $n_j \leq 20$ [17]

$$\kappa_{tr} = k\big((0.38n_{jmax}+1)(kr_{min})^{-1} + 0.03(kr_{min})\big) \quad (17)$$

which implies that it can be used for antennas with a diameter of up to 3λ. The maximum value for the degree of the spherical mode expansion, n_{jmax} in (17), should be chosen to provide the desired accuracy. The criterion given in [18] can be applied to obtain this value

$$n_{jmax} = \left[kr_{min} + 0.045\sqrt[3]{kr_{min}}(-Ptr)\right] \quad (18)$$

where Ptr is the relative truncated (i.e., excluded) power in decibel with respect to the total radiated power due to the series truncation. Since very close interactions take place when the minimum spheres overlap, a larger degree should be retained in the spherical wave expansion, compared to the case of nonoverlapping minimum spheres. In this work, we have verified that very good results are obtained by choosing Ptr equal to -130 dB, which provides an intermediate value between those suggested in [19] and in [16]. However, the accuracy of the results obtained by using the value of κ_{tr} provided by (17) can be improved in some cases by using a higher value, as it will be shown in Section III.

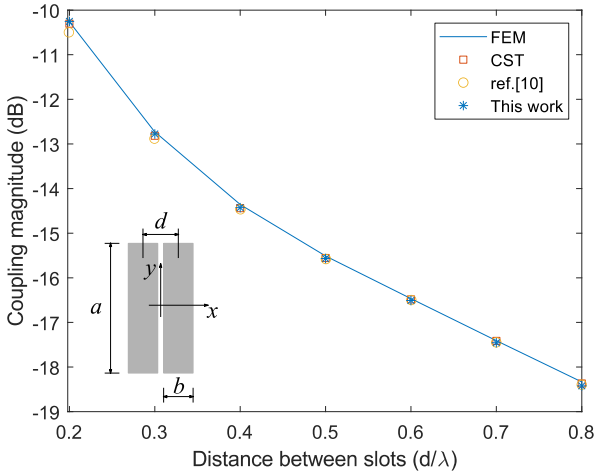

Fig. 3. Coupling magnitude between rectangular slots in terms of the distance between axes. Slot dimensions are specified in the text. The inset shows a top scaled view of the coupled slot antennas and the parameter definitions for the geometry. At this drawing scale, $d = 0.2\lambda$ and the working frequency is 10 GHz.

On the other hand, it should be noted that, in the range of application discussed in [17] and given at the beginning of this section, it is true that $\kappa_{tr} > k$. Therefore, within these limits of use, the entire spectrum of propagating plane waves (where the propagation constant of plane waves jk_z is imaginary and then $\kappa < k$) is always taken into account, and the spectrum of evanescent plane waves is truncated. Consequently, only evanescent plane waves that are attenuated more rapidly are no longer considered. This truncation avoids contributions from the diverging spherical wave expansion in the near-field zone [17].

III. Results

In this section, some antenna array examples analyzed with strongly overlapped spheres will be shown.

A. Study of Two Slots

The first example consists of two rectangular slots with dimensions $a = 2.286$ cm, $b = 0.508$ cm, filled with air, on an infinite ground plane and analyzed at 10 GHz. This example was previously proposed in [10], where an analysis method based on the calculation of the GSM of an antenna in terms of equivalent dipoles was presented. As mentioned above, that method also allowed the study of antennas with overlapped spheres.

Fig. 3 shows the magnitude of mutual coupling, obtained with the method proposed in this work, compared with the results obtained by using an in-house finite element method (FEM) [20], CST, and the previous result from [10]. In this case, the truncated value for the integral $\kappa_{tr} = 3k$ was used, with $n_{max} = 10$. The proposed method provides a coupling magnitude that agrees with the value obtained with FEM and CST, whereas the value from [10] deviates starting from a distance between centers of 0.4λ. Specifically, for a

TABLE I

COUPLING MAGNITUDES FOR SLOTS OF FIG. 3

S parameters	FEM	CST	This work ($\kappa_{tr} = 3k$)	This work ($\kappa_{tr} = 2k$)
S_{11} (dB)	-5.61	-5.55	-5.64	-5.67
S_{21} (dB)	-10.26	-10.39	-10.25	-10.27

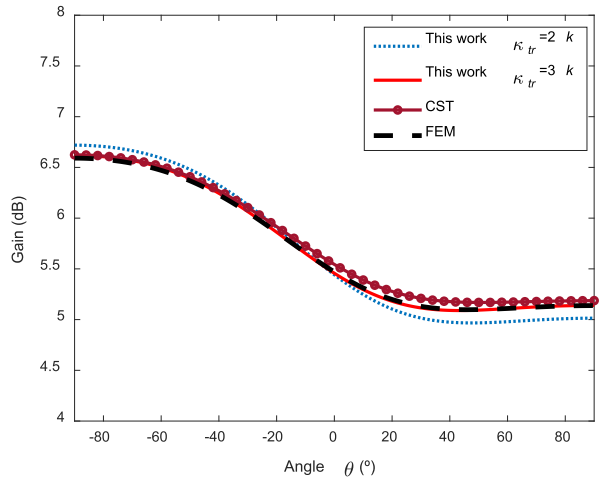

Fig. 4. Gain pattern at $\varphi = 0°$ for the two rectangular slots shown in the inset of Fig. 3, calculated with $d = 0.2\lambda$ at 10 GHz.

TABLE II

S-PARAMETERS FOR THE ARRAY OF FIG. 5(A) (CENTRAL ELEMENT IS #2)

S parameters (dB)	S_{11}	S_{12}	S_{21}	S_{13}	S_{22}
[11]	-9.56	-7.64	-7.93	-16.01	-5.97
CST	-10.29	-7.75	-7.75	-15.40	-6.44
FEM	-10.30	-7.79	-7.79	-15.39	-6.41
This work	-10.30	-7.79	-7.79	-15.43	-6.41

separation distance equal to 0.2λ (see the inset of Fig. 3), values for S_{11} and S_{21} are shown in Table I.

For this same case, Fig. 4 shows the calculated gain in the plane of the array ($\varphi = 0°$), feeding just one antenna. The maximum difference between our method and FEM is 0.03 dB for $\kappa_{tr} = 3k$ and 0.13 dB for $\kappa_{tr} = 2k$. As shown in Table I, S-parameters are accurately obtained also with $\kappa_{tr} = 2k$, the value calculated with (17) given in [17]. However, the radiation pattern slightly deviates from the reference pattern.

B. Study of Three Coupled Monopoles on an Infinite Ground Plane

The following example consists of three monopoles 15 mm long ($\lambda/4$), with diameter 1.5 mm, and separated 0.2λ between centers, as shown in Fig. 5. The monopoles are fed with a 50 Ω coaxial connector and analyzed at 5 GHz.

This case was also studied previously with the equivalent dipole model in [11]. Table II shows a comparison of S-parameters calculated with several methods for a separation of 0.2λ between monopoles. As can be observed, our results agree well with FEM and CST simulation, but the method used in [11] shows a small error mainly in reflection S-parameters and provides also different values for S_{12} and S_{21}.

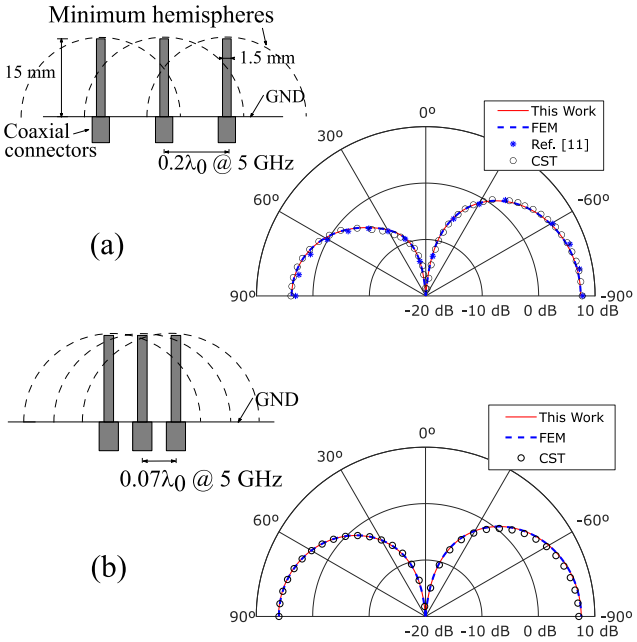

Fig. 5. Gain pattern (cut at $\varphi = 0°$) for three monopoles separated (a) 0.2λ and (b) 0.07λ when feeding the leftmost monopole only. The insets at the left show the array geometries including the overlapping hemispheres for each case. Drawings are provided at scale in order to stand out the strong overlapping of case (b) when compared to (a).

TABLE III

S-PARAMETERS FOR THE ARRAY OF FIG. 5(B) (CENTRAL ELEMENT IS #2)

S parameters (dB)	S_{11}	S_{12}	S_{13}	S_{22}
FEM	-7.31	-6.02	-8.53	-6.41
CST	-7.19	-6.01	-8.32	-6.41
This work	-7.39	-5.97	-8.50	-6.54

Fig. 5(a) shows the array gain when one lateral antenna is fed. As can be seen, results obtained with the present method fit very well to CST and FEM results, whereas those of [11] separate from them at angles near the ground plane, where the gain reaches a relative maximum.

The array of three monopoles of Fig. 5(a) solved in [11] implies only overlapping between contiguous monopoles. In order to show the capabilities of the present method, the array of Fig. 5(b) has been studied, where the distance between the monopoles axes is just 0.07λ, which considers also a strong overlap between lateral spheres. This can be observed in Fig. 5(b), where the distance between the closest edges of coax feeders is 0.0125λ approximately. For this case, the results shown in Table III have been obtained, that still compare very well with those of CST and FEM.

Fig. 5(b) also shows the gain pattern for the array of three monopoles for 0.07λ. The results of FEM simulations agree very well with the proposed method, whereas CST simulations deviate only slightly.

Finally, Fig. 6 shows the rms function error of S-parameters in terms of $\bar{\kappa}_{tr} = \kappa_{tr}/k$ and the maximum n used, taking the

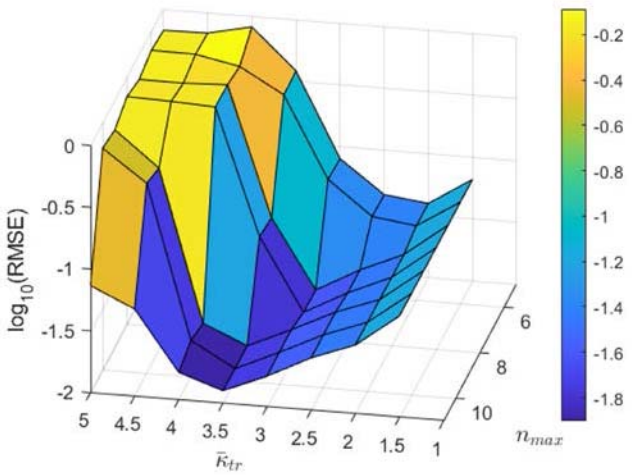

Fig. 6. RMS error as a function of the integral truncated value ($\bar{\kappa}_{tr}$) and the maximum n used (n_{max}). The array analyzed was the three monopoles of Fig. 5 with elements separated 0.07λ.

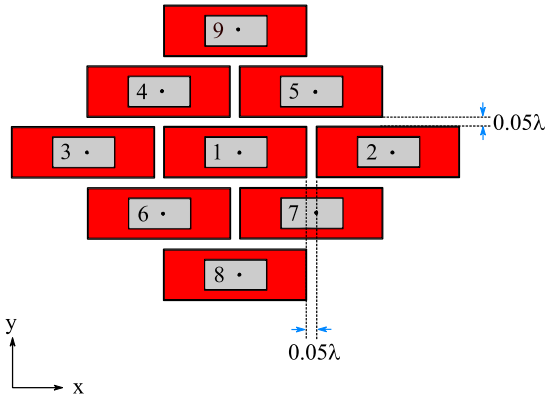

Fig. 7. Top view of an antenna array with nine cavity-backed patch antennas. Dielectric is shown in red. Every feeding point is depicted for each patch. Separation between elements is 0.05λ at the working frequency. Antenna dimensions can be found in [10].

FEM results as a reference

$$\mathrm{RMSE} = \frac{\sqrt{\sum_{i=1}^{3}\sum_{j=1}^{3}|\mathrm{S}_{ij}^{TW} - \mathrm{S}_{ij}^{FEM}|^2}}{3}. \tag{19}$$

This kind of convergence for these variables agrees well with the one reported in [17] for the calculation of spheroidal particles scattering with minimum overlapping spheres. Although the previous results have been obtained with $\kappa_{tr} = 3k$ and $n_{max} = 8$, it can be observed that an optimum value is roughly achieved with $\kappa_{tr} = 3.5k$ and n_{max} near to 9, respectively, very close to $\kappa_{tr} = 3k$ used in the present example. For this case, the formula provided in [17] given by (17) leads to κ_{tr} values of approximately 2.6 and 2.8, for n_{max} values of 8 and 9, respectively, which are slightly below the one used in this work.

C. Array of Nine Cavity-Backed Patch Antennas

In the following example, an array of nine cavity-backed patch antennas tightly packed is analyzed with the proposed methodology of this work. Geometrical data for the patch antenna can be found in [10]. This array arrangement is shown in Fig. 7, where the separation between parallel sides of each patch antenna is 0.49 cm, equivalent to 0.05λ at the working frequency. In this case, adjacent antennas whose centers have a different y-coordinate cannot be separated with an orthogonal plane to the axial direction, so that propagation of plane waves will be in the direction of y-axis.

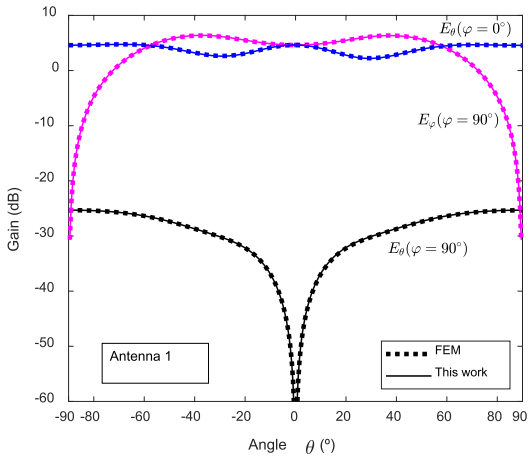

Fig. 8. Gain pattern simulated with the proposed method and FEM for the array of Fig. 7 when only antenna 1 is fed. Two cuts are represented for E_θ and E_φ.

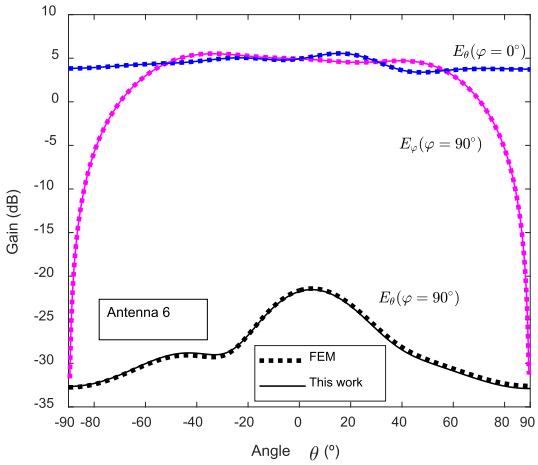

Fig. 9. Gain pattern simulated with the proposed method and FEM for the array of Fig. 7 when only antenna 6 is fed. Two cuts are represented for E_θ and E_φ.

Figs. 8 and 9 show E_θ and E_φ gains for $\varphi = 0°$ and $\varphi = 90°$, when antenna 1 and 6 are respectively fed. A good agreement between results obtained with the present method and FEM simulations can be observed, with maximum differences of 0.04 dB in copolar and 0.25 dB in cross-polar components.

Tables IV and V show the magnitudes of reflection and coupling S-parameters of antennas 1 and 6. As can be observed, results fit well when compared to FEM simulations. They were obtained for $\kappa_{tr} = 3k$ and $n_{max} = 10$. If $\kappa_{tr} = 2.1k$ is used, instead of the previous value, as predicted by (17) given in [17], the results are very similar.

D. Array of Thirty-Six Dielectric Resonator Antennas

This last example consists of an array of thirty-six dielectric resonator antennas and linear polarization, with sequential

TABLE IV
S-PARAMETERS FOR ANTENNA 1 OF FIG. 7

S param. (dB)	This work	FEM
S_{11}	-24.47	-24.68
S_{21}	-19.18	-19.11
S_{31}	-18.65	-18.59
S_{41}	-17.09	-17.10
S_{51}	-17.15	-17.17
S_{61}	-17.09	-17.11
S_{71}	-17.15	-17.16
S_{81}	-21.92	-21.94
S_{91}	-21.92	-21.95

TABLE V
S-PARAMETERS FOR ANTENNA 6 OF FIG. 7

S param. (dB)	This work	FEM
S_{61}	-17.09	-17.11
S_{62}	-23.82	-23.72
S_{63}	-16.97	-16.96
S_{64}	-21.73	-21.75
S_{65}	-28.83	-28.87
S_{66}	-26.00	-26.23
S_{67}	-19.03	-18.94
S_{68}	-17.08	-17.08
S_{69}	-26.72	-26.72

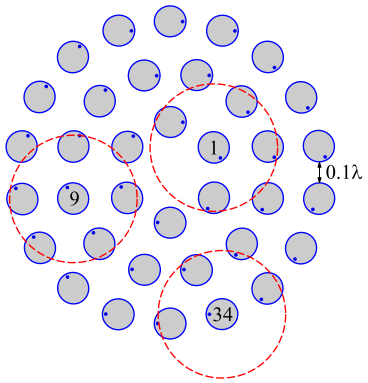

Fig. 10. Top view of a thirty-six dielectric resonator antenna array. The array has three rings where elements are placed. Array dimensions are given in the text. Element dimensions are specified in [21], for the highest resonator case. Minimum separation is 0.1λ at the working frequency. Dashed circles represent the basis of minimum hemispheres surrounding several elements.

rotation at 60° steps by sectors in order to obtain circular polarization, located in three circular rings. Rings radii are 0.96429, 1.92858, and 2.89287 cm. Simulations were done at 9.835 GHz, the resonant frequency obtained with FEM for an isolated antenna. At this frequency and the above dimensions, the minimum horizontal spacing between adjacent elements is just 0.1λ.

The resonant dielectric antenna with the highest height analyzed in [21] has been chosen as the element of the array. Fig. 10 shows the array geometry as well as the corresponding circle of the minimum hemisphere surrounding an antenna of each ring. As shown, each element has a strong overlapping with several other elements.

In Fig. 11, the gain pattern obtained for $\varphi = 0°$ and $\varphi = 90°$ is shown, when antennas of the inner ring are fed with the same amplitude and phase equal to the rotation angle.

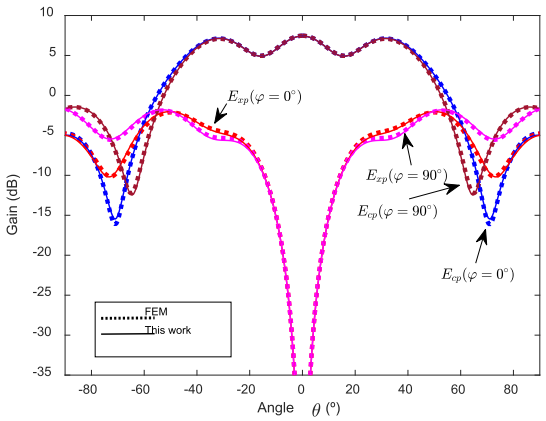

Fig. 11. Gain patterns for the array of Fig. 10 when the inner antennas are fed with unitary amplitude and phase the rotation angle. Results for cross- and copolar components are shown for $\varphi = 0°$ and $\varphi = 90°$.

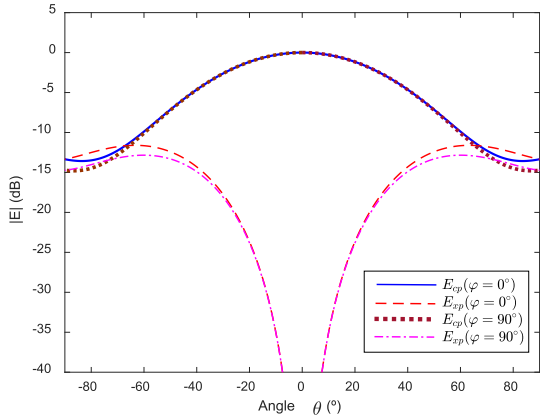

Fig. 12. Radiation patterns for the same conditions of Fig. 11, without the effect of coupling between elements. Results for cross- and copolar components are shown for $\varphi = 0°$ and $\varphi = 90°$.

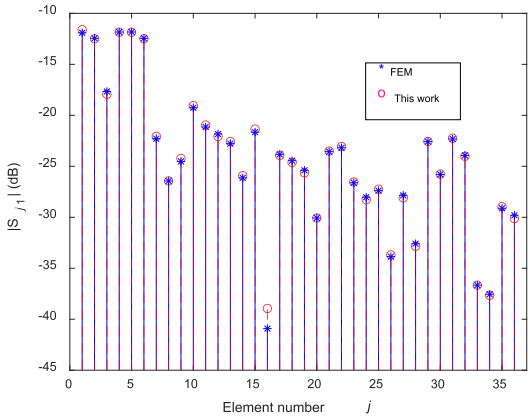

Fig. 13. S_{j1} parameter magnitudes for the array of Fig. 10.

The results are compared to FEM simulations, showing a good agreement, just differing 0.2 dB, except at levels less than −10 dB, where they deviate as much as 0.7 dB. The influence of mutual coupling on the array performance is shown in Fig. 12, where the same cuts of Fig. 11 are considered without mutual coupling.

Reflection (S_{jj}) and coupling (S_{ij}) magnitudes are shown in Figs. 13–15 for the array of Fig. 10. As previously found, results agree well with FEM simulations. Maximum differ-

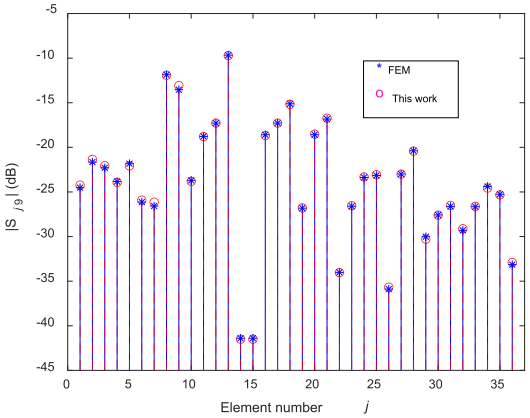

Fig. 14. S_{j9} parameter magnitudes for the array of Fig. 10.

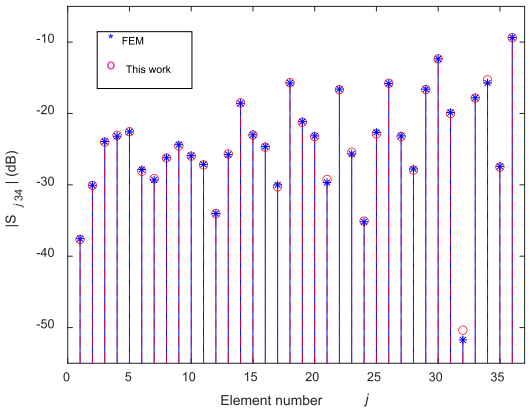

Fig. 15. S_{j34} parameter magnitudes for the array of Fig. 10.

ences below 0.5 dB were obtained, except for small coupling magnitudes. Simulations were carried out with $\kappa_{tr} = 3k$ and $n_{max} = 10$. If the value $\kappa_{tr} = 2k$, as predicted by (17) given in [17], was used, then differences with FEM simulations would grow up to 1.7 dB. For this case, radiation pattern results deviate from FEM simulations by 0.4 dB except for levels below -10 dB, where differences reach 1 dB.

For this array, with the greatest number of elements of all the examples presented in this work, it is worth to compare simulation times. FEM simulation took 2 h and 24 min with a 4 606 400 elements mesh for the whole array, whereas the proposed method in this work required only 1 min and 31 s for an isolated antenna simulated with a 154 000 elements mesh. The response of the whole array was obtained in 31 s by computing (3a) and (3b) using MATLAB 2019b.

IV. Conclusion

In this article, we have proposed a fast method for the full-wave analysis of antenna arrays, which is capable of dealing with tight-packed antennas since it is based on transformation between spherical and plane vector waves. In this way, the use of the GSM finite array formulation has been extended to the case of elements with strongly overlapping minimum spheres, which was a limitation of that method. In addition, properties of the translation coefficients have been provided that strongly speed up their computation.

The method is fast and reliable when compared with full FEM simulations or commercial software. Convergence is guaranteed by using established criteria.

References

[1] J. Bruning and Y. Lo, "Multiple scattering of EM waves by spheres part I—Multipole expansion and ray-optical solutions," *IEEE Trans. Antennas Propag.*, vol. AP-19, no. 3, pp. 378–390, May 1971.

[2] M. I. Mishchenko, G. Videen, V. A. Babenko, N. G. Khlebtsov, and T. Wriedt, "T-matrix theory of electromagnetic scattering by particles and its applications: A comprehensive reference database," *J. Quantum Spectrosc. Radiat. Transf.*, vol. 88, pp. 357–406, Aug. 2004.

[3] M. I. Mishchenko, "Comprehensive thematic T-matrix reference database: A 2017-2019 update," *J. Quantum Spectrosc. Radiat. Transf.*, vol. 242, pp. 1–9, Feb. 2020, doi: 10.1016/j.jqsrt.2019.106692.

[4] J. E. Hansen, Ed., *Spherical Near-Field Antenna Measurements*. London, U.K.: Peter Peregrinus Ltd., 1988.

[5] J. Rubio, M. A. Gonzalez, and J. Zapata, "Generalized-scattering-matrix analysis of a class of finite arrays of coupled antennas by using 3-D FEM and spherical mode expansion," *IEEE Trans. Antennas Propag.*, vol. 53, no. 3, pp. 1133–1144, Mar. 2005.

[6] J. Rubio, J. Corcoles, and M. A. G. de Aza, "Inclusion of the feeding network effects in the generalized-scattering-matrix formulation of a finite array," *IEEE Antennas Wireless Propag. Lett.*, vol. 8, pp. 819–822, 2009.

[7] J. Rubio, A. G. Garcia, R. G. Alcala, J. Garcia, and Y. Campos-Roca, "Simultaneous use of addition theorems for cylindrical and spherical waves for the fast full-wave analysis of SIW-based antenna arrays," *IEEE Trans. Antennas Propag.*, vol. 67, no. 12, pp. 7379–7386, Dec. 2019.

[8] S. Stein, "Addition theorem for spherical wave functions," *Quart. Appl. Math*, vol. 19, no. 1, pp. 15–24, 1961.

[9] O. R. Cruzan, "Translational addition theorem for spherical vector wave functions," *Quart. Appl. Math*, vol. 20, no. 1, pp. 33–40, 1962.

[10] J. F. Izquierdo, J. Rubio, and J. Zapata, "Antenna-generalized scattering matrix in terms of equivalent infinitesimal dipoles: Application to finite array problems," *IEEE Trans. Antennas Propag.*, vol. 60, no. 10, pp. 4601–4609, Oct. 2012.

[11] J. F. Izquierdo, J. Rubio, and J. Zapata, "Spherical-waves-based analysis of arrays of volumetric antennas with overlapping minimum spheres," *IEEE Antennas Wireless Propag. Lett.*, vol. 11, pp. 1296–1299, 2012.

[12] Y. Adane, A. Gati, M.-F. Wong, C. Dale, J. Wiart, and V. F. Hanna, "Optimal modeling of real radio base station antennas for human exposure assessment using spherical-mode decomposition," *IEEE Antennas Wireless Propag. Lett.*, vol. 1, pp. 215–218, 2002.

[13] A. Boström, G. Kristensson, and S. Ström, "Transformation properties of plane, spherical and cylindrical scalar and vector wave functions," in *Field Representations Introduction to Scattering*. Amsterdam, The Netherlands: Elsevier, 1991, ch. 4, pp. 165–210.

[14] D. Theobald, A. Egel, G. Gomard, and U. Lemmer, "Plane-wave coupling formalism for t -matrix simulations of light scattering by nonspherical particles," *Phys. Rev. A, Gen. Phys.*, vol. 96, no. 3, pp. 1–8, Sep. 2017, doi: 10.1103/PhysRevA.96.033822.

[15] J. I. Echeveste, J. Rubio, M. A. G. de Aza, and C. Craeye, "Pattern synthesis of coupled antenna arrays via element rotation," *IEEE Antennas Wireless Propag. Lett.*, vol. 16, pp. 1707–1710, 2017.

[16] C. Cappellin, O. Breinbjerg, and A. Frandsen, "Properties of the transformation from the spherical wave expansion to the plane wave expansion," *Radio Sci.*, vol. 46, pp. 1–16, Feb. 2008.

[17] A. Egel, Y. Eremin, T. Wriedt, D. Theobald, U. Lemmer, and G. Gomard, "Extending the applicability of the T-matrix method to light scattering by flat particles on a substrate via truncation of sommerfeld integrals," *J. Quant. Spectrosc. Radiat. Transf.*, vol. 202, pp. 279–285, Nov. 2017.

[18] F. Jensen and A. Frandsen, "On the number of modes in spherical wave expansions," in *Proc. 26th AMTA*, Stone Mountain Park, GA, USA, Oct. 2004, pp. 489–494.

[19] W. J. Wiscombe, "Improved Mie scattering algorithms," *Appl. Opt.*, vol. 19, no. 9, pp. 1505–1509, 1980. 10.1364/AO.19.001505.

[20] J. Rubio, J. Arroyo, and J. Zapata, "Analysis of passive microwave circuits by using a hybrid 2-D and 3-D finite-element mode-matching method," *IEEE Trans. Microw. Theory Techn.*, vol. 47, no. 9, pp. 1746–1749, Sep. 1999.

[21] R. Chair, A. A. Kishk, and K.-F. Lee, "Comparative study on the mutual coupling between different sized cylindrical dielectric resonators antennas and circular microstrip patch antennas," *IEEE Trans. Antennas Propag.*, vol. 53, no. 3, pp. 1011–1019, Mar. 2005.

Jesús Rubio was born in Talavera de la Reina, Toledo, Spain, in 1971. He received the Ingeniero de Telecomunicación degree in 1995 and the Ph.D. degree in 1998, both from the Universidad Politécnica de Madrid, Madrid, Spain.

He is a Professor with the School of Technology, Cáceres, Spain. His current research interests are in the application of the finite element method and modal analysis to antennas and passive microwave circuits problems.

Rafael Gómez-Alcalá (Member, IEEE) was born in Córdoba, Spain, in 1965. He received the Ingeniero de Telecomunicación degree and the Ph.D. degree in telecommunication from the University of Vigo, Vigo, Spain, in 1990 and 1996, respectively.

In 1999, he moved to the University of Extremadura, Badajoz, Spain, where he is currently an Associate Professor with the School of Technology, Cáceres, Spain. His research interests include microwave filters and antenna design.